



Lasers in Manufacturing Conference 2015

Pulsed Laser Surface Pre-Treatment of Aluminium to Join Aluminium-Thermoplastic Hybrid Parts

André Heckert^{a*}, Christian Singer^b, Michael F. Zaeh^a

^a*Institute for Machine Tools and Industrial Management (iwb), Technische Universität München, Boltzmannstrasse 15, 85748 Garching, Germany*

^b*Technische Universität München, Boltzmannstrasse 15, 85748 Garching, Germany*

Abstract

Thermal joining of aluminium and thermoplastics by laser radiation is promising. To obtain a high joint strength, the metal surface is pre-treated prior to bonding. Laser surface pre-treatment was used to pre-treat aluminium specimens in this study. The laser process allows a flexible processing of surface structures in the range from nanoscopic to macroscopic scale. An infrared pulsed single-mode fibre laser with a pulse width of 100 ns was used to form a microscopic structure on the specimens. The surface was overlain by a porous oxide layer. This oxide layer differs significantly from the natural passivation layer. It is assumed that the oxide layer contributes to a great extent to the cohesion between the aluminium and the thermoplastic material. This study focuses on the generation of the microscopic structure with an oxide layer and its influence on the resulting joint strength between aluminium and thermoplastics. To create a variety of surface topologies, different cumulative energies were applied to the specimens. The resulting surface topologies were investigated by scanning electron microscopy, the surface enlargement was characterized using gas adsorption, the surface roughness was quantified by laser scanning microscopy, and the surface chemistry was analysed by X-ray photoelectron microscopy. The oxide layer was removed from the structured specimens by an etching process to compare both samples, with and without a porous oxide layer. Subsequently, joints of the laser structured aluminium and the thermoplastics were prepared by thermal joining. The joint strength was measured by tensile shear tests and correlated to the surface areas, roughness values, and laser energies for etched and non-etched aluminium specimens to identify the influence of the microscopic structure and the oxide layer.

Keywords: Laser, Surface Pre-Treatment, Aluminium-Thermoplastic Hybrid Joint

* Corresponding author. Tel.: +49-(0)89-289 15589; fax: +49-(0)89-289 15555.
E-mail address: Andre.Heckert@iwb.tum.de

1. Motivation

Lightweight construction is a main objective of the automotive industry. As a consequence, hybrid joints made of fibre reinforced thermoplastics and lightweight metals such as aluminium are gaining in importance. In this context, thermal joining is currently under investigation by several researchers (Amend et al. 2014, Schricker et al. 2014, Heckert & Zaeh 2014), because high joint strengths can be reached and the thermoplastic joining partner is directly used as an adhesive. The heat input, which is necessary for joining, can be applied by friction, induction, ultrasonics or radiation such as laser radiation (Flock 2011). In this regard, the laser beam radiation is an outstanding tool for joining since it allows for an efficient and flexible energy input.

There are two principals for joining metal-plastic hybrids via laser radiation: Transmission joining and heat-conduction joining. Using the process of transmission joining, the laser beam is transmitted through the laser-transparent plastic material and heats the metal surface. Subsequently, the plastic material melts and wets the surface structures of the metal. For plastics which are not transparent to the laser beam radiation, e.g. for glass fibre reinforced thermoplastics, heat-conduction joining can be applied. In this configuration, the laser beam is radiated onto the outer metal surface. Due to heat conduction, the energy is transferred to the metal-plastic interface, which leads to the melting of the plastic joining partner and the wetting of the metal surface. The joint is established as soon as the thermoplastic re-solidifies.

To obtain load bearing metal-plastic joints by thermal joining, the metal has to be pre-treated prior to bonding (Heckert & Zaeh 2014). Again, the laser can be used for this task with outstanding results. To pre-treat the metal surfaces, continuous wave as well as pulsed laser sources are used. In most studies regarding thermoplastic-metal connections, kerfs or craters in the macroscopic regime were produced, using both laser sources (Amend et al. 2014, Roesner 2014, Rodríguez et al. 2014, Heckert & Zaeh 2014). The laser-based surface structures enable the plastic material to infiltrate the metal cavities and lead to a significant increase in the joint strength when compared to samples with other (e.g. abrasive blasting) or no surface pre-treatment (Wirth et al. 2014). An alternative approach for pre-treating the surface was investigated by Hose (2008) and Rechner (2012) for adhesively bonded metal joints. The authors used a pulsed infrared laser beam source to uniformly structure the aluminium surface with overlapping laser pulses. Yet, this laser structuring process and the associated binding mechanisms have not been investigated for the application in thermoplastics-to-metal connections.

2. Background: Pulsed laser surface pre-treatment

Rechner (2012) and Hose (2008) used pulsed infrared laser systems with pulse widths in the regime of nanoseconds to process different aluminium alloys. By applying laser pulses in this regime, the metal surface is molten and/or partially evaporated, depending on the absorbed laser energy. Microscopic surface structures, which are overlain by a newly formed porous oxide layer, can be created by the correct setting of laser parameters such as: Laser power, pulse repetition rate, pulse duration, hatch distance, and number of repetitions.

To investigate the influence of the oxide layer on the joint properties, Hose (2008) and Rechner (2012) employed different process gases, such as oxygen, helium or nitrogen, and ambient air while structuring the aluminium surfaces. The experiments revealed a correlation between the tensile shear strength and the thickness of the oxide layer. According to Rechner (2012), the adhesive infiltrated the oxide layer during the joining process and formed an interlayer between the joining partners.

Moreover, the investigations of Rechner (2012) showed an increase of the surface roughness with an increasing laser energy per area. A specific amount of energy caused the formation of a rough surface with nodular structures which originated from the melting and the re-solidification of the aluminium. The surface area was doubled at its highest value in comparison to untreated surfaces.

Besides the increase in surface area, the laser structuring process modifies the chemical composition of the aluminium. Hose (2008) and Rechner (2012) identified a chemical cleaning effect by employing Energy Dispersive X-ray analysis and X-ray Photoelectron Spectroscopy (XPS). The oxygen in the surface layer, which indicates the generation of oxide on the structured surface, was increased. Depending on the process gas which was used, the magnitude of oxide increased with the amount of oxygen in the gas. Moreover, the content of carbon, which is related to the amount of surface contaminations, was reduced by up to one third in comparison to an untreated surface (Rechner 2012).

3. Experimental setup

3.1. Materials

The aluminium alloy AlMgSi1 (EN AW-6082) and a glass fibre reinforced thermoplastic laminate (PA6-GF66) were used in this study to manufacture the hybrid aluminium-thermoplastic joints.

3.2. Laser surface structuring of the aluminium

The aluminium was pre-treated by a pulsed single-mode Yb-fibre laser Powerline F20 from the Rofin SINAR Laser GmbH. This laser has a wavelength of 1064 nm, a pulse width of 100 ns and an average laser power of 20 W. The laser beam was focused to a spot diameter of approximately 50 μm and the pulses were applied in an overlapping configuration with an equal hatch distance in vertical and horizontal direction. The remaining parameters for surface structuring are listed in Table 1.

Table 1. Process parameters for surface structuring of the aluminium

| Parameter | | | | |
|---------------------------------|-----|----|----|----|
| Repetition rate in kHz | 20 | | | |
| Pulse energy in mJ | 0.5 | 1 | | |
| Hatch distance in μm | 10 | 20 | 30 | |
| Number of repetitions | 1 | 2 | 5 | 10 |

The total amount of energy which has been applied to the surface during the pre-treatment was varied in terms of cumulative energy. The cumulative energy E_{cum} is defined by the number of repetitions n_{rep} , the pulse energy E_p and the hatch distance l_{hd} :

$$E_{cum} = \frac{4 \cdot E_p}{\pi \cdot l_{hd}^2} \cdot n_{rep} \quad (1)$$

All samples were produced in ambient atmosphere. Thus, a porous oxide layer was built on the surface of the metal. To separately investigate the influence of the oxide layer and the microscopic structure, the oxide layer was removed by an etching process.

A solution of 10 % caustic soda was used to etch the samples. Due to varying laser parameters, which lead to different oxide layer thicknesses, it was necessary to adjust the etching duration for each laser structure. This was done to ensure a removal of the oxide layer while keeping the microscopic structure unmodified. All samples were examined by scanning electron microscopy (SEM) to identify remaining porous oxides on the

surface. In Fig. 1a) an SEM picture with a porous oxide layer is displayed. The oxide layer can be identified by the fuzzy film on the microscopic structure. In contrast, an etched surface with a dissolved microscopic structure is shown in Fig. 1c). An etching duration of 60 seconds was chosen for the study, since it resulted in an unaffected microscopic structure and an absence of the porous oxide layer (Fig. 1d).

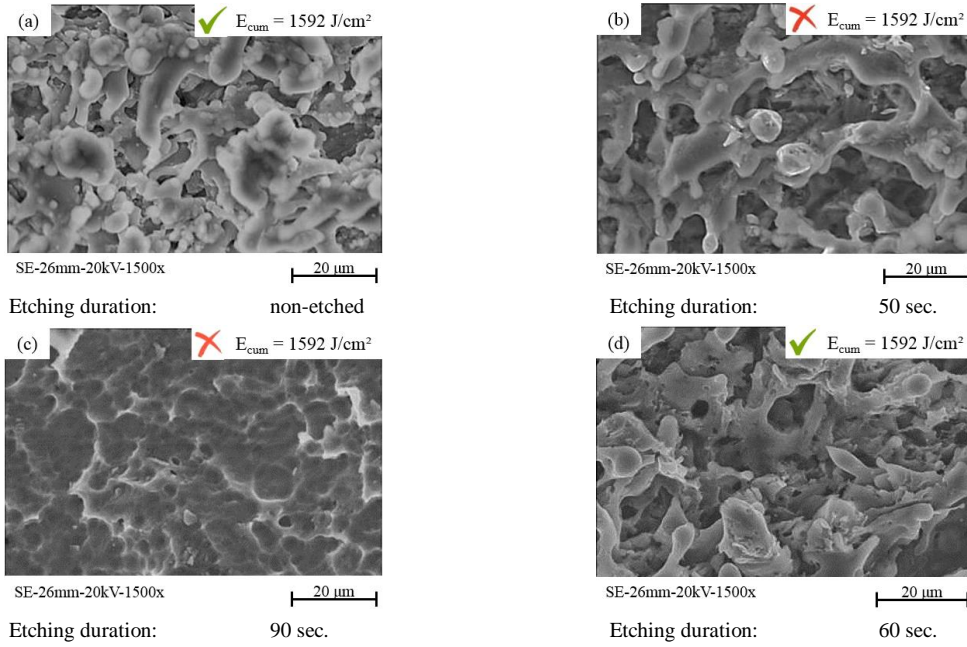


Fig. 1. SEM-photographs of an etching study for the laser pre-treated aluminium at 1592 J/cm^2 with (a) oxide covered structures for the non-etched surface; (b) a surface with oxidic residuals; (c) a dissolved microscopic structure and (d) an oxide free surface after the etching process

3.3. Thermal joining of the metal to the plastic material

The aluminium-thermoplastic specimens were bonded by laser-based heat conduction joining. The experimental setup is shown in Fig. 2. An overlapping length of $12.5 \pm 0.25 \text{ mm}$ was chosen and the specimens were compressed with a force of 175 N during the joining process. A single-mode Yb-fibre laser with a scanning optics was used to irradiate the aluminium surface with an elliptic trajectory in the size of $20 \text{ mm} \times 6 \text{ mm}$ for 300 times at a laser power of 800 W . The overlapping area was determined by measuring the overlapping length and the sample width for all specimens after joining.

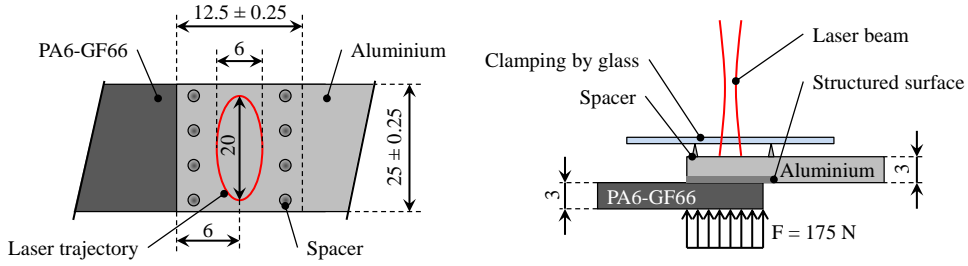


Fig. 2. Experimental setup for thermal joining of laser structured aluminium AlMgSi1 with glass fibre reinforced PA6-GF66 by laser radiation

The tensile shear strength was determined according to DIN EN 1465:2009 using a tensile rate of 2 mm / min. The specimens were tested by a universal tensile testing machine Z020 from Zwick. Three samples of each combination of laser parameters were tested and the average was calculated.

3.4. Surface analysis of laser structured aluminium by gas adsorption

The increase in surface area of the laser pre-treated aluminium surface was measured by gas adsorption (BET: Brunauer-Emmett-Teller theory). This method, which is described in DIN ISO 9277:2010, is introduced as a new approach to quantify the increase in surface area caused by the laser structuring.

For the BET-measurement, krypton is passed over the laser structured aluminium specimens in a cylindrical test chamber. Due to a cooling below the saturation vapour pressure of the krypton, it is possible to measure the amount of adsorbed gas on the surface which leads to a change in the pressure rate. The relation between the adsorbed gas and the pressure rate is described by the adsorption isotherm. According to the adsorption isotherm, a defined number of molecules cover the surface with a monolayer of krypton molecules. Consequently, the surface size S can be calculated using the amount of molecules n_m , the required space A_{Mol} for each molecule, and the Avogadro-term N_A (Stieß 2009):

$$S = A_{Mol} \cdot n_m \cdot N_A \quad (2)$$

4. Results and discussion

4.1. Analysis of the surface topology by laser scanning microscopy

The surface roughness for the etched and non-etched surfaces was measured with a Laser Scanning Microscope (LSM) VK9710 from Keyence. The mean roughness index was calculated by the average of five roughness lines positioned in the measured surface area. The results are shown in Fig. 3. Each line in the plot is associated with a certain hatch distance and pulse energy. The cumulative energy was varied by modifying the number of repetitions.

The mean roughness increases with the cumulative energy. This result is in accordance with the findings of Rechner (2012). A higher cumulative energy results in more molten material, a higher share of ablation and in consequence in a higher roughness. By employing the same amount of cumulative energy, the samples treated with a pulse energy of 1.0 mJ exhibit a higher roughness in comparison to the samples with 0.5 mJ. Furthermore, the number of repetitions affects the mean roughness significantly for a pulse energy of 1.0 mJ and less

significantly for 0.5 mJ. The pulse energy of 0.5 mJ might not be enough to create a significant amount of melt. The surface roughness was not significantly increased and the material was rather ablated when several repetitions with a pulse energy of 0.5 mJ were applied.

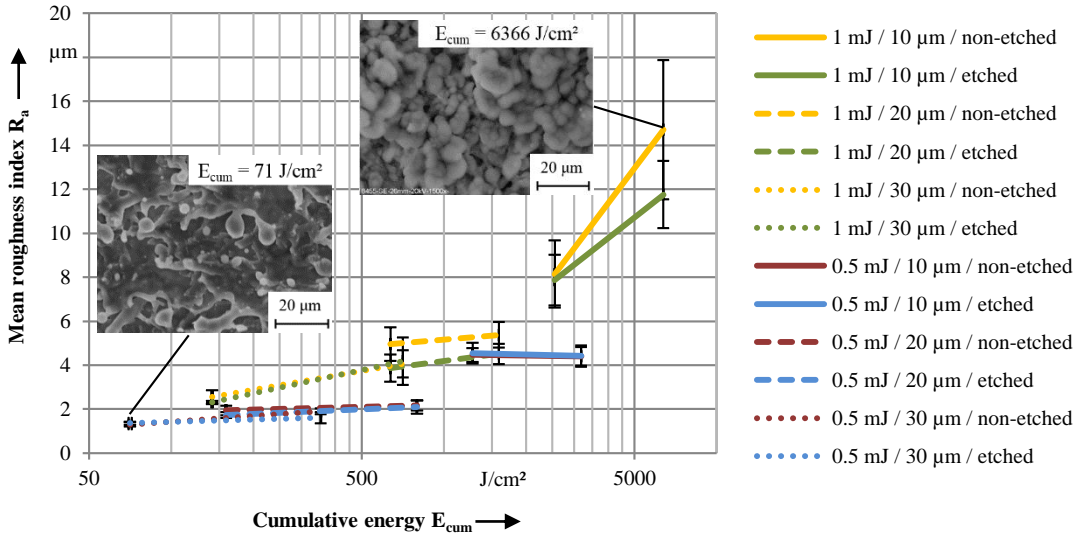


Fig. 3. LSM-measured mean roughness index R_a for laser pre-treated surfaces depending on the cumulative energy with SEM-photographs

The results of the LSM measurement reveal a deviation of the measured mean roughness between the etched surfaces compared to the non-etched surfaces for high roughness values (e.g. 1.0 mJ / 10 μm, 1.0 mJ / 20 μm both etched and non-etched). Furthermore, higher standard deviations can be observed with high cumulative energies. In contrast, the roughness values of the remaining parameters are in good accordance. As shown by the SEM pictures of Fig. 1, nodular structures with undercuts in a great extent are generated with the laser process. For reference, a three-dimensional analysis with the LSM of two laser structured surfaces is shown in Appendix A. The cumulative energy was 1273 J/cm² and 71 J/cm², respectively. A comparison between Appendix A1 and Fig. 1a) reveals, that it is not possible to detect the undercuts with LSM. As a consequence, a roughness measurement via LSM can only describe the surface topology of the laser structured specimens to a limited extent. Furthermore, the accordance in the roughness of etched and non-etched samples indicates that it is not possible to distinguish the roughness values by the existence of the oxide layer. To determine the influence of the microscopic structure and the oxide layer it is necessary to employ other methods. In this regard, the gas adsorption was introduced to quantify the enlargement in the surface area and the XPS was used for a chemical investigation of the surface.

4.2. Analysis of the surface topology by gas adsorption

As described in section 3.4, the gas adsorption was chosen to measure the surface enlargement of the aluminium with surface structuring. The cumulative energy and the graphs were derived in the same way as it was done for Fig. 3. The result of the BET measurement in Fig. 4 shows a significant increase in the surface area for an enhanced cumulative energy for etched and non-etched specimens. Applying a maximum cumulative

energy of about 6366 J/cm², a surface area for the non-etched specimens of 569 cm² was measured. This surface area is 247 times larger than the non-treated aluminium surface with 2.3 cm².

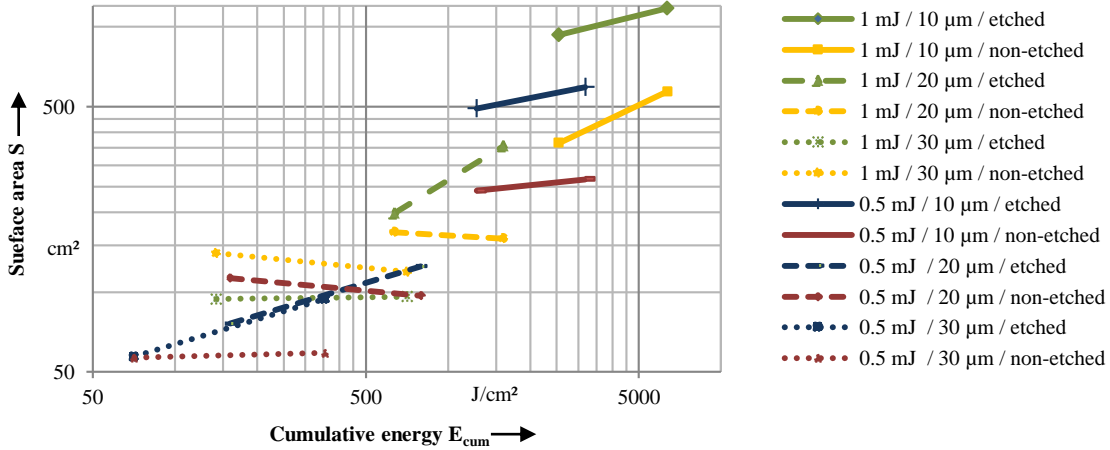


Fig. 4. Surface size S measured by BET for laser pre-treated surfaces depending on the cumulative laser energy of etched and non-etched specimens

In accordance with the roughness measurements (see Fig. 3), the number of repetitions caused a less significant change in surface area for low cumulative energies and a significant change for high cumulative energies. In contrast to the findings of the roughness analysis, the etched samples exhibit a higher surface area than the non-etched samples. A decrease in the cumulative energy results in smaller differences between the quantified surface area of etched and non-etched specimens. For some of the samples subjected to a low cumulative energy the behaviour was inverted – the surface area was smaller for the etched samples. However, in these cases the differences were smaller with a maximum deviation of 50 cm². The results indicate that etching with caustic soda modifies the microscopic structure (cf. Fig. 1). For high cumulative energies longer etching durations were chosen according to the findings of the SEM analysis. In this case, the oxide layer was removed but the etching caused also a modification of the surface structure. Thus, an increase in surface area was obtained. However, this result is contrary to the roughness measurement in which the measured roughness was the same or smaller for the etched samples.

4.3. Analysis of the chemical composition of the aluminium surface by XPS

XPS spectra were recorded with a Physical Electronics Versa Probe II using an Al $K\alpha_{1,2}$ x-ray source ($h\nu = 1486.6$ eV) in the monochromatic mode at 24.6 W at a pressure below $1 \cdot 10^{-6}$ Pascal. All data was collected and stored with 128 channel mode detection. The spectrometer was operated with a spot size of 100 μm and a Pass Energy of 23.5 eV resulting in an energy resolution of 0.1 eV.

The results of the element distribution on the surface are listed for two processing parameters and the non-treated substrate material in Table 2. For each parameter an etched and a non-etched specimen was investigated. In general, mainly carbon (C1s), oxygen (O1s), and aluminium (Al2p) were detected on the aluminium surface. Magnesium (Mg2) and Calcium (Ca2p) were observed in small quantities. After laser pre-treating, the carbon content was significantly reduced, the oxygen and the aluminium content were significantly increased. The carbon content is associated with a contamination of the surface. Thus, the surface of both samples, etched and non-etched, was cleaned by the laser pre-treatment. According to Rechner (2012), Hose (2008) and

Dimogerontakis et al. (2005) the increase in oxygen content is linked to the formation of the oxide layer. As a consequence, a higher oxygen content indicates more oxide on the surface. Moreover, the oxide content increases with the cumulative energy. When comparing the element distribution for etched and non-etched samples, no significant difference was observed when identical processing parameters were applied. Only a slight increase in carbon content was detected for the etched specimens.

Table 2. Results of the XPS-measurement for laser-structured etched and non-etched surfaces

| Cum. energy (J/cm ²) | Etching | Parameters | C1s (at%) | O1s (at%) | Al2p (at%) | Mg2s (at%) | Ca2p (at%) |
|----------------------------------|---------|---------------------|-----------|-----------|------------|------------|------------|
| - | Yes | Non-treated | 69.9 | 23.0 | 3.4 | 2.3 | 1.4 |
| - | No | Non-treated | 66.2 | 23.5 | 4.9 | 3.8 | 1.7 |
| 6366 | Yes | 20 W, 10 μm, 5 rep. | 18.0 | 54.0 | 21.9 | 4.9 | 1.3 |
| 6366 | No | 20 W, 10 μm, 5 rep. | 15.0 | 55.5 | 24.0 | 5.3 | 0.2 |
| 1591 | Yes | 20 W, 20 μm, 5 rep. | 22.7 | 48.2 | 24.0 | 3.0 | 2.0 |
| 1591 | No | 20 W, 20 μm, 5 rep. | 19.2 | 50.8 | 24.8 | 5.1 | 0.1 |

However, Fig. 5 shows a modification in the detailed aluminium spectra for the etched specimens. These samples exhibit a splitting of the aluminium peak. According to Barr et al. (1994) binding energies between 74.0 eV and 75.7 eV are assigned to the aluminium oxide Al₂O₃. The peak A is consequently associated with different oxide species of Al₂O₃ or hydroxides. However, a detailed distinction between oxide or hydroxide is not possible since the peaks interfere (Rechner 2012). For the etched specimens, a second peak B was observed. This peak is usually found with thin oxide layers and can be associated with the bare aluminium (Barr et al. 1994).

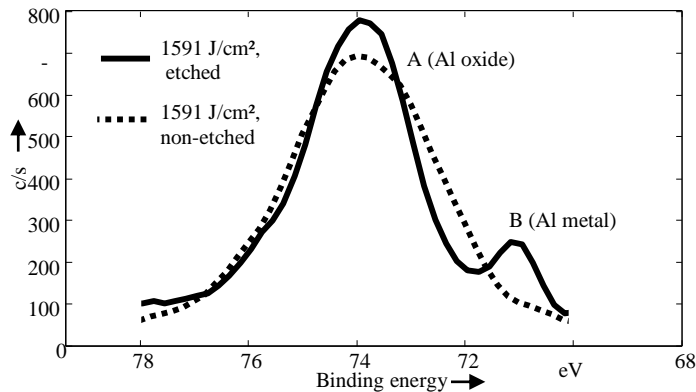


Fig. 5. Detailed aluminium spectrum: Metal and oxide peaks (etched surface); only oxide peak (non-etched surface)

The results indicate, that by etching the specimens, the oxide layer was successfully removed since bare aluminium was detected. In contrast, the non-etched samples exhibit a thicker oxide layer which correlates with the cumulative energy.

4.4. Mechanical strength of the aluminium-thermoplastic joint

The results of the tensile shear test are shown in Fig. 6. Each graph in the plot is associated with a specific hatch distance and pulse energy. The cumulative energy was varied by modifying the number of repetitions.

The tensile shear strength correlates with the cumulative energy. Furthermore, a threshold value was identified. In comparison to the roughness and gas adsorption analysis (see Fig. 3 and Fig. 4), where an increase of the cumulative energy led to a continuous increase in roughness, a threshold in joint strength is reached at approximately 2000 J/cm². No significant further increase in joint strength was achieved by an increased cumulative energy. The strength reached a plateau at a level of about 23.0 - 26.0 N/mm². From an economic point of view, this threshold value has to be determined since an increase in cumulative energy correlates with a higher processing time.

In contrast to the roughness and gas adsorption measurements, no significant influence in the number of repetitions on the joint strength for both, low pulse and high pulse energies, was detected. The shear strength was not increased with the number of repetitions, but it increased with the amount of cumulative energy adjusted by the hatch distance and the pulse energy up to the threshold value. A maximum shear strength of approximately 26 N/mm² was measured for a pulse energy of 1 mJ, a hatch distance of 10 μm and the non-etched surfaces at a cumulative energy of 6366 J/cm². According to the surface analysis, this surface exhibits a largely undercut structure with high roughness, high surface area, and a thick oxide layer (see Fig. 3). It is indicated that these characteristics lead to an enhanced mechanical adhesion of aluminium and thermoplastic polymer.

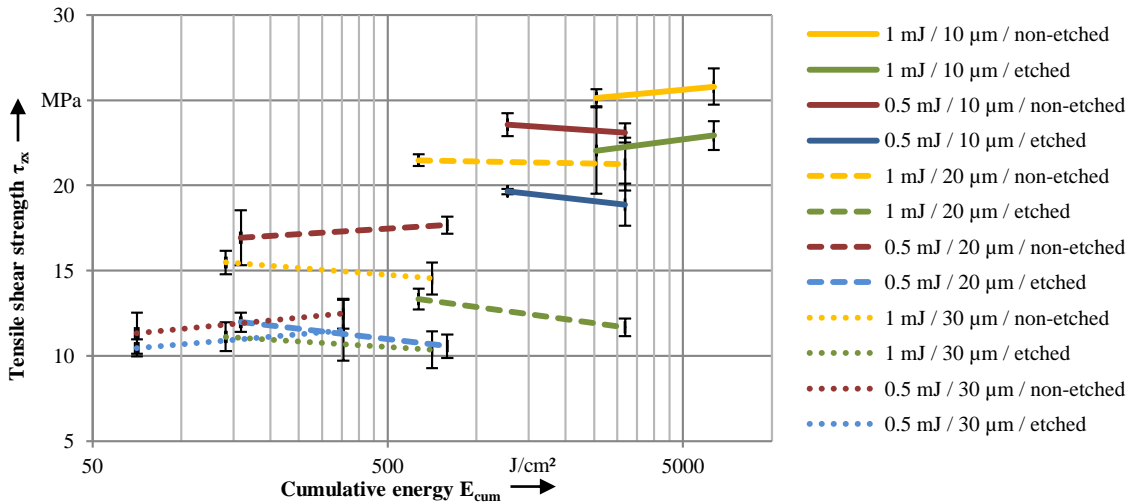


Fig. 6. Tensile shear strength for the aluminium-thermoplastic joints depending on the hatch distance, laser pulse energy and for etched and non-etched surfaces.

In tensile shear tests, the strength with etched surfaces was lower than with non-etched surfaces, even though a higher surface area was detected by gas adsorption. The results show a significant reduction in shear strength caused by the etching process and the removal of the oxide layer. The mean shear strength of all samples with non-etched surfaces is 19.1 N/mm²; the mean shear strength of all samples with etched surfaces is 13 N/mm², approximately one third less. The influence of the etching process on the joint strength was low for low cumulative energies. The mean difference between etched and non-etched specimens with an energy of less

than 500 J/cm² was only 1 N/mm². In contrast, a significant influence of the etching process was detected for parameters with a hatch distance between 10 μm and 20 μm and higher cumulative energies. This behaviour can be explained by the extended etching times, which result in a modification of the surface area according to the BET analysis.

The results presented in Fig. 6, and in particular the differences in shear strength caused by the oxide layer, are in accordance to the findings of Rechner (2012) and Hose (2008). The authors, who pre-treated the surfaces with different process gases, also determined a decrease in strength for the surfaces with a lower amount of oxide. Rechner (2012) described the formation of an interlayer consisting of both, adhesive and oxide, which caused best the joint properties. This phenomenon seems to occur at joints made of aluminium and thermoplastic polymers, as well. The polymer wets the porous oxide layer and therefore the adhesion is enhanced. Yet, the microscopic structure with the nodular undercuts seems to affect the joint strength significantly. In conclusion, both, the microscopic structure and the porous oxide layer are crucial for creating strong and load bearing aluminium-thermoplastic joints.

5. Conclusion and outlook

- High joint strengths of up to 26 N/mm² for the hybrid joint made of aluminium and fibre reinforced polyamide were achieved by employing the laser surface structuring process with a subsequent laser based thermal joining.
- The SEM analysis show that laser surface pre-treatment of aluminium results in a microscopic structure and a porous oxide layer. The oxide layer could be removed by a subsequent etching process.
- This finding was confirmed by the XPS-analysis. Furthermore, the porous oxide layer which was created on the surface of the aluminium thickens with an increase in cumulative energy.
- The microscopic roughness of the surface, measured by LSM, correlates with the cumulative energy. In general, an increase in cumulative energy leads to a higher roughness. Moreover, it could be shown, that the LSM was not able to detect the porous oxide layer or the nodular undercuts created by the laser structuring.
- The BET analysis reveals a surface enlargement of up to 247-times for the non-etched laser structured surfaces in comparison to the untreated surface. A linear correlation of cumulative energy and surface area was observed. In contrast to the roughness measurements, a higher surface area was detected for the majority of the etched samples. This was associated with the etching processes which lead to a modification of both microscopic structure and oxide layer. However, the results indicate that the BET analysis is, in contrast to roughness measurements, an adequate tool for achieving quantitative evidence about the surface morphology of laser structured aluminium specimens.
- The mechanical experiments show that the joint strength correlates with the cumulative energy up to a threshold value of around 2000 J/cm². From this point on, the strength reached a plateau at 23 N/mm² to 26 N/mm². The inclinations of the graphs indicate that the load bearing fraction of the surface structure is mainly built with the first repetition. A further increase in number of repetitions does not change the joint strength significantly. Moreover, the joint strength is significantly reduced by the etching process, although an increase in surface area was measured within the BET analysis. In conclusion, the results suggest that both microscopic structure and oxide layer are crucial for creating a high joint strength for thermoplastic-aluminium joints.
- Investigations of Rechner (2012) indicate that the influence of the surface morphology is particularly high when the specimens are submitted to ageing and environmental influences. As a consequence, further research is planned to address this issue for the application with thermoplastic-aluminium joints.

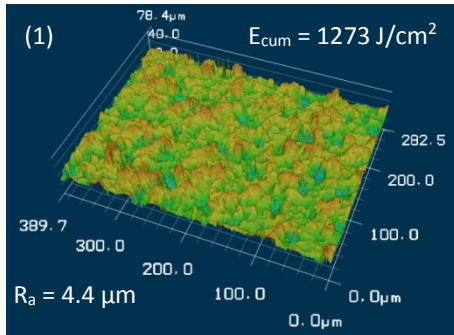
Acknowledgements

The results presented in this paper were gathered within the research project “NexHOS”, funded by the German Federal Ministry for Economic Affairs and Energy (BMWi). The authors thankfully acknowledge its financial support.

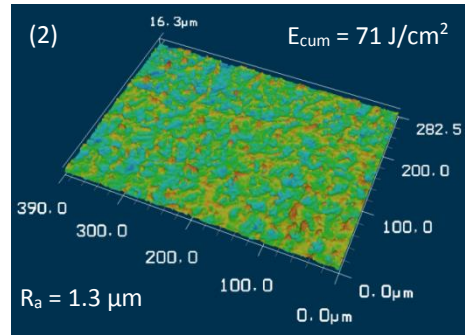
References

- Amend, P.; Mohr, C.; Roth, S., 2014. Experimental Investigations of Thermal Joining of Polyamide Aluminum Hybrids Using a Combination of Mono- and Polychromatic Radiation. In: *Physics Procedia* 56, pp. 824–834.
- Barr, T.L., Seal, S., Mei Chen, L., Chang Kao, C., 1994. A New Interpretation of the Binding Energies in X-Ray Photoelectron Studies of Oxides. In: *Thin Solid Films* 253, pp. 277-284.
- Dimogerontakis, Th., Oltra, R., Heintz, O., 2005. Thermal Oxidation Induced during Laser Cleaning of an Aluminium-Magnesium Alloy. In: *Appl. Phys. A* 81 (6), pp. 1173–1179.
- DIN EN 1465:2009, July 2009. Adhesives - Determination of Tensile Lap-Shear Strength of Bonded Assemblies.
- DIN ISO 9277:2010, January 2014. Determination of the Specific Surface Area of Solids by Gas Adsorption - BET Method.
- Flock, D., 2011. Wärmeleitungsfügen hybrider Kunststoff-Metall-Verbindungen. PhD Thesis. Aachen.
- Heckert, A.; Zaeh, M. F., 2014. Laser Surface Pre-treatment of Aluminium for Hybrid Joints with Glas Fibre Reinforced Thermoplastics. In: *Physics Procedia* 56, pp. 1171–1181.
- Hose, R., 2008. Laseroberflächenvorbehandlung zur Verbesserung der Adhäsion und Alterungsbeständigkeit von Aluminiumklebungen. PhD Thesis, Aachen: Shaker Verlag.
- Rechner, R., 2012. Laseroberflächenvorbehandlung von Aluminium zur Optimierung der Oxidschichteigenschaften für das strukturelle Kleben. PhD Thesis, 1st Edition. München: Dr. Hut.
- Rodríguez-Vidal, E., Lambarri, J., Soriano, C., Sanz, C., Verhaeghe, G., 2014. A Combined Experimental and Numerical Approach to the Laser Joining of Hybrid Polymer-Metal Parts. In: *Physics Procedia* 56, pp. 835-844.
- Roesner, A., 2014. Laserbasiertes Fügeverfahren zur Herstellung von Kunststoff-Metall-Hybridbauteilen. PhD Thesis, Aachen, : Fraunhofer Verlag, Fraunhofer ILT.
- Schricker, K., Stambke, M., Bergmann, J. P., Brätigam, K., Henckell, P., 2014. Macroscopic Surface Structures for Polymer-Metal Hybrid Joints manufactured by Laser Based Thermal Joining. In: *Physics Procedia* 56, pp. 782-790.
- Stieß, M., 2009. Partikeltechnologie. 3rd Edition. Berlin: Springer.
- Wirth, F. X., Zaeh, M. F., Krutzlinger, M., Silvanus, J., 2014. Analysis of the Bonding Behavior and Joining Mechanism during Friction Press Joining of Aluminum Alloys with Thermoplastics. In: *Procedia CIRP* 18, pp. 215–220.

Appendix A. LSM-measurements of laser pre-treated aluminium surfaces for different cumulative energies



Pulse energy: 1 mJ
Hatch distance: 10 μm
Repetitions: 2
Etching duration: non-etched



Pulse energy: 1 mJ
Hatch distance: 30 μm
Repetitions: 1
Etching duration: non-etched